



Since January 2020 Elsevier has created a COVID-19 resource centre with free information in English and Mandarin on the novel coronavirus COVID-19. The COVID-19 resource centre is hosted on Elsevier Connect, the company's public news and information website.

Elsevier hereby grants permission to make all its COVID-19-related research that is available on the COVID-19 resource centre - including this research content - immediately available in PubMed Central and other publicly funded repositories, such as the WHO COVID database with rights for unrestricted research re-use and analyses in any form or by any means with acknowledgement of the original source. These permissions are granted for free by Elsevier for as long as the COVID-19 resource centre remains active.



ELSEVIER

Contents lists available at ScienceDirect

Virus Research

journal homepage: [www.elsevier.com/locate/virusres](http://www.elsevier.com/locate/virusres)

## Effects of hypervariable regions in spike protein on pathogenicity, tropism, and serotypes of infectious bronchitis virus

Dan Shan<sup>a</sup>, Shouguo Fang<sup>b</sup>, Zongxi Han<sup>a</sup>, Hui Ai<sup>a</sup>, Wenjun Zhao<sup>a</sup>, Yuqiu Chen<sup>a</sup>, Lei Jiang<sup>a</sup>, Shengwang Liu<sup>a,\*</sup>

<sup>a</sup> Division of Avian Infectious Diseases, State Key Laboratory of Veterinary Biotechnology, Harbin Veterinary Research Institute, The Chinese Academy of Agricultural Sciences, Harbin 150026, China

<sup>b</sup> Agricultural School, Yangtze University, 266 Jingmi Road, Jingzhou City, Hubei Province 434025, China

### ARTICLE INFO

#### Keywords:

Hypervariable region  
Infectious bronchitis virus  
Infectious clone  
Recombinant IBV  
Reverse genetic vaccine

### ABSTRACT

To study the roles of hypervariable regions (HVRs) in receptor-binding subunit S1 of the spike protein, we manipulated the genome of the IBV Beaudette strain using a reverse genetics system to construct seven recombinant strains by separately or simultaneously replacing the three HVRs of the Beaudette strain with the corresponding fragments from a QX-like nephropathogenic isolate ck/CH/LDL/091022 from China. We characterized the growth properties of these recombinant IBVs in Vero cells and embryonated eggs, and their pathogenicity, tropism, and serotypes in specific pathogen-free (SPF) chickens. All seven recombinant IBVs proliferated in Vero cells, but the heterogenous HVRs could reduce their capacity for adsorption during *in vitro* infection. The recombinant IBVs did not significantly increase the pathogenicity compared with the Beaudette strain in SPF chickens, and they still shared the same serotype as the Beaudette strain, but the antigenic relatedness values between the recombinant strain and Beaudette strain generally decreased with the increase in the number of the HVRs exchanged. The results of this study demonstrate the functions of HVRs and they may help to develop a vaccine candidate, as well as providing insights into the prevention and control of IBV.

### 1. Introduction

IBV primarily replicates in the epithelial surface of the respiratory tract, although some strains are nephropathogenic (Cavanagh, 2003). IBV infections reduce egg production, quality, and hatchability, as well as increasing the feed conversion ratio and carcass condemnation in slaughterhouses. Thus, infectious bronchitis causes severe economic losses in the poultry industry worldwide.

The enveloped IBV belongs to the genus *Coronavirus*, family Coronaviridae, order Nidovirales (Cavanagh, 2003). The main structural protein is the spike (S) glycoprotein, which comprises a divergent S1 subunit and conserved S2 subunit (de Groot et al., 1987; Shil et al., 2011). The S1 subunit contains the receptor-binding domain (Wickramasinghe et al., 2011), and it carries virus-neutralizing and serotype-specific determinants. The S1 domain exhibits high sequence diversity, where 20%–25% (even up to 50%) of the amino acids differ within the S1 subunit among IBV serotypes. After comparing the S1 subunit from a number of distinct IBV isolates, a previous study defined particularly variable segments at the amino terminus of the S1 subunit as hypervariable regions (HVRs) (Kusters et al., 1989).

The HVRs possibly account for the antigenicity and serotypic variation, and evidence indicates that five neutralizing peptides mainly mapped onto the S1 subunit are co-located within the HVRs (Cavanagh et al., 1992, 1988; Moore et al., 1997; Niesters et al., 1987). In addition, the HVRs are possibly associated with receptor binding. It has been reported that the critical amino acids for attachment of the M41 spike overlap with a HVR in the S1 subunit (Promkuntod et al., 2014). Thus, the HVRs may affect the tropism, serotype, and pathogenicity of IBV, and it is important to elucidate their biological functions.

Previous studies applied forward genetics methods to determine the roles of the HVRs by characterizing their phylogenetically closely related isolates with mutations in other parts of the IBV genome, but it is difficult to establish a precise model for further analysis based on these studies. Thus, in this study, we manipulated the IBV Beaudette genome by reverse genetics to exchange the HVRs in the Beaudette strain with those in ck/CH/LDL/091022 in order to precisely determine their biological functions. We also explored the possibility of developing a reverse genetic vaccine candidate cultured in Vero cells to provide protection from the prevalent field strains. The results of this study contribute to our understanding of the prevention and control of IBV.

\* Corresponding author.

E-mail addresses: [swliu@hvri.ac.cn](mailto:swliu@hvri.ac.cn), [liushengwang@caas.cn](mailto:liushengwang@caas.cn) (S. Liu).

## 2. Materials and methods

### 2.1. Cells and viruses

Vero cells were maintained in Dulbecco's modified Eagle's medium (Gibco, Grand Island, NY, USA) supplemented with 10% fetal bovine serum (Sigma-Aldrich, Saint Louis, MO, USA), penicillin (100 units/ml), and streptomycin (100 µg/ml) at 37°C with 5% carbon dioxide. The ck/CH/LDL/091022 strain was isolated from H120-vaccinated chickens with renal lesions in 2009 (Liu et al., 2013). The Beaudette strain was routinely propagated in Vero cells (Liu et al., 1995, 1998; Tay et al., 2012) and the 50% tissue culture infection dose (TCID<sub>50</sub>) of the viral stock was calculated using 96-well plates with 10-fold serial dilutions. The 50% egg infection dose (EID<sub>50</sub>) of the viral stock was determined by inoculating 10-fold dilutions into groups of 9-day-old embryonated chicken eggs.

### 2.2. Recovery of infectious recombinant IBVs

Five fragments spanning the entire IBV genome were obtained by RT-PCR from Vero cells infected with the IBV Beaudette strain, as described previously (Fang et al., 2007). The three HVRs in the isolate ck/CH/LDL/091022 were identified based on alignments of the amino acid sequences, as described previously (Zhang et al., 2015). The sequences of the IBV cDNA covering the three HVRs in the S gene were replaced separately or simultaneously with those from ck/CH/LDL/091022, and subsequently ligated into the full-length IBV cDNA (Fig. 1a and Table 1). Full-length transcripts generated *in vitro* were introduced into Vero cells by electroporation. IBV N gene transcripts were also generated to enhance the efficiency of viral recovery. Total RNA was prepared from the electroporated Vero cells or infected allantoic liquid. Viral RNA replication was investigated based on RT-PCR of negative-strand genomic RNA (Tan et al., 2006). The S gene in the recovered IBV clones (third passage in Vero cells and embryonated eggs) was amplified by RT-PCR and subsequently confirmed by DNA sequencing analysis. The gene was characterized during the third passage of viruses in specific pathogen-free (SPF) embryonated eggs or Vero cells. The seven rescued recombinant IBVs were designated as rHVR I, rHVR II, rHVR III, rHVR I/II, rHVR I/III, rHVR II/III, and rHVR I/II/III.

### 2.3. Growth kinetics of the recombinant IBVs

To determine the growth kinetics of the rescued recombinant IBVs, a dose of 100 × EID<sub>50</sub> was inoculated into the allantoic cavities of 9-day-old embryonated eggs, and the allantoic fluid was harvested from three eggs in each group at 12, 24, 36, 48, and 60 h post-inoculation, where the fluids from three eggs were pooled for EID<sub>50</sub> determination with three replicates. Vero cells were infected with Beaudette and recombinant IBVs, and three wells were harvested at 4, 8, 12, 16, 24, and 36 h post-infection. Viral stocks were prepared by freezing/thawing the cells three times to determine the TCID<sub>50</sub> with three replicates for each time.

### 2.4. Immunofluorescent (IF) staining

IBV infected cells cultured in six-well plates were washed with phosphate-buffered saline (PBS), fixed with 4% paraformaldehyde for 15 min, and permeabilized with 0.2% Triton X-100 for 10 min. IF staining was performed with a monoclonal antibody 6D10 against IBV N protein (Han et al., 2013) and subsequently with FITC-conjugated anti-mouse IgG (Sigma-Aldrich). Cells were examined by fluorescence microscopy.

### 2.5. Pathogenicity test

All of the animal experimental procedures were approved by the

Ethical and Animal Welfare Committee of Heilongjiang Province, China (License no. SQ20160408).

We randomly assigned 150 7-day-old SPF layer chickens to 10 groups, *i.e.*, the seven recombinant strains, Beaudette, ck/CH/LDL/091022, and PBS groups. There were 15 SPF chickens in each group. The challenge strain (10<sup>5</sup> × EID<sub>50</sub> per bird) was applied *via* the intranasal and ocular routes. The clinical signs were monitored in 10 randomly selected challenged birds from each group, and the morbidity and mortality rates were recorded daily. We evaluated the challenged chickens blindly for respiratory rates at 5 days after challenge. Signs were scored as 0 = absent, 1 = mild, 2 = moderate, or 3 = severe. At 5 days after IBV challenge, the other five birds in each group were killed humanely using carbon dioxide over inhalation, followed by exsanguination. The cranial third of the trachea, lungs, kidneys, and cecum tonsils were collected, partly fixed in formalin, and embedded in paraffin. Longitudinal 5-µm sections were stained with hematoxylin-eosin (H&E stain). The mucosal thickness, deciliation, goblet cells, and lymphocytes scores for the tracheal mucosa were evaluated blindly and scored from 1 to 5 based on their severity (*i.e.*, normal, mild, moderate, marked, and severe) (van Ginkel et al., 2015). Moreover, viral shedding was quantified in the oropharyngeal secretions from 10 infected chickens at 4, 8, 12, 16, and 20 days after challenge by real-time RT-PCR (Jones et al., 2011).

### 2.6. *In vivo* Tissue tropism

The tissues collected at 5 days post-IBV challenge, *i.e.*, tracheas, lungs, kidneys, and cecum tonsils, were also subjected to immunohistochemistry (IHC) using monoclonal antibody 6D10, as described previously (de Wit et al., 2011; Xu et al., 2016). Viral loads in selected tissues were determined based on IBV RNA detection by real-time RT-PCR, as described previously (Zhao et al., 2017).

### 2.7. Cross-virus neutralization assay

The seven IBV recombinant strains, Beaudette, and ck/CH/LDL/091022 were analyzed in cross-virus neutralization tests. Sera against the IBV strains were prepared as previously described (Zhang et al., 2015). In the virus neutralization tests, sera were serially diluted two times with sterile PBS and mixed with 200 × EID<sub>50</sub> or TCID<sub>50</sub> for the IBV strains. The two-way cross-neutralization test between the Beaudette and recombinant IBVs was performed in Vero cells. After incubation for 1 h at 37 °C, the virus-serum mixtures were cultured in 96-well microplates for 5 days. We could not detect the replication with ck/CH/LDL/091022 in Vero cells, so the neutralization tests were performed in 9-day-old SPF embryonated eggs to confirm whether the serotypes of the recombinant IBVs belonged to ck/CH/LDL/091022. The end-point titer for each serum sample was calculated using the Reed–Muench method. Antigenic relatedness values were calculated (Archetti and Horsfall et al., 1950; Wade and Faragher, 1981).

### 2.8. Adsorption and internalization assessments using a cellular enzyme-linked immunosorbent assay (cELISA)

The cELISA protocol used in this study is similar to the conventional ELISA. The viral solution for each strain was serially diluted two times with sterile PBS and coated on the plate. Standard curves were drawn according to the standard ELISA method. Vero cells were cultured overnight in 96-well microplates (Corning, USA) (10<sup>5</sup> cells/well). For the adsorption assay, each strain was incubated in cells at a multiplicity of infection (MOI) of 1 for 1 h at 4 °C with three replicates (Fang et al., 2010; Sun et al., 2017). After two washes with PBS, the microplates were fixed with methanol and 1% hydrogen peroxide for 30 min, and then permeabilized with 0.2% Triton X-100 for 10 min at room temperature. Next, the microplates were washed three times and blocked with 8% skim milk for 30 min at room temperature. After washing three

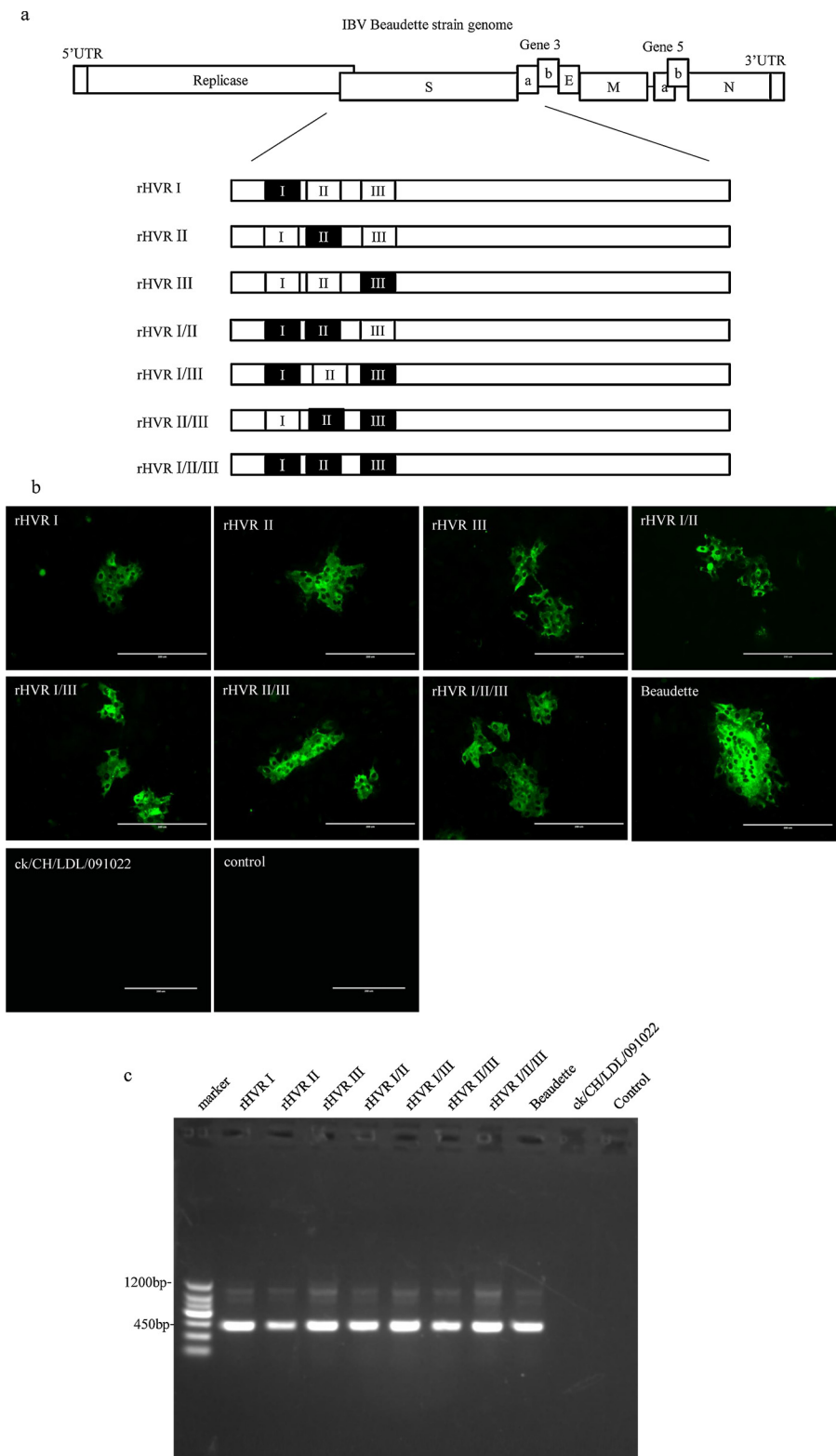


**Fig. 1.** Recovery of the recombinant IBVs from cells. (a) Diagram showing the organization of the genomes in the recombinant IBVs. The genome structure of the IBV Beaudette strain is shown in the white rectangle. Regions coding for the hypervariable regions (HVRs) in the IBV strain ck/CH/LDL/091022 are shown in the black rectangle. (b) Immunofluorescent staining of Vero cells infected with the recombinant IBVs. The cells were infected with the recombinant IBVs and the two parental strains. At 24 h post-infection, the cells were fixed and stained with the monoclonal antibody against IBV N protein. (c) Detection of the viral RNA in Vero cells by RT-PCR. Total RNA was extracted from Vero cells electroporated with full-length transcripts at 48 h post-electroporation. RT-PCR was used to amplify the regions corresponding to the 5'-terminal 415 bp and 1010 bp of subgenomic mRNA 4 and 3, respectively.

times, the microplates were incubated with the primary mouse monoclonal antibody 6D10 for 1 h at 37 °C. A similar procedure was then performed where the plates were incubated for 40 min with the peroxidase-conjugated anti-mouse IgG. Peroxidase substrate solution (TMB; Sigma-Aldrich) was added and the plates were developed in darkness. The color reaction was stopped with stop solution (Sigma-Aldrich) and the absorbance was read at 630 nm. For the internalization assay, cells were seeded into 96-well microplates and inoculated with

each strain for 1 h at 37 °C. After incubation, the cells were washed twice with PBS, before treating the infected cells with citrate buffer for 1 min to inactivate the adsorbed but not internalized virus. The cells were washed with PBS to remove the citrate buffer. The cELISA process was performed as described above. The cELISA results were expressed as the relative viral load adsorbed or internalized into cells relative to the Beaudette control.

**Table 1**  
Summary of mutations in HVRs introduced into the Beaudette strain.

Name	Amino acid sequences in the S1 subunit of spike protein <sup>a</sup>		
	HVR I (positions 50–86)	HVR II (positions 104–138)	HVR III (positions 272–291)
Beaudette	VNISSEFNAGSSSGCTVGIHGGRRVNVASSIAMTAP	FSDTTVFVTHCYKHGGCPITGMLQQNFIRVSAMKN	FIFHNETGANPNPSGVQNIQ
ck/CH/LDL/091022	VNSTNYTSNAGSASECTVGVIKDVYNQSAASIAMTAP	FSEITVFVTHCYSSGTGSCPTGMIARDHIRISAMKN	FTFTNVSTAQPNSGGVSTFH
rHVR I	VNSTNYTSNAGSASECTVGVIKDVYNQSAASIAMTAP	FSDTTVFVTHCYKHGGCPITGMLQQNFIRVSAMKN	FIFHNETGANPNPSGVQNIQ
rHVR II	VNISSEFNAGSSSGCTVGIHGGRRVNVASSIAMTAP	FSEITVFVTHCYSSGTGSCPTGMIARDHIRISAMKN	FIFHNETGANPNPSGVQNIQ
rHVR III	VNISSEFNAGSSSGCTVGIHGGRRVNVASSIAMTAP	FSDTTVFVTHCYKHGGCPITGMLQQNFIRVSAMKN	FTFTNVSTAQPNSGGVSTFH
rHVR I/II	VNSTNYTSNAGSASECTVGVIKDVYNQSAASIAMTAP	FSEITVFVTHCYSSGTGSCPTGMIARDHIRISAMKN	FIFHNETGANPNPSGVQNIQ
rHVR I/III	VNSTNYTSNAGSASECTVGVIKDVYNQSAASIAMTAP	FSDTTVFVTHCYKHGGCPITGMLQQNFIRVSAMKN	FTFTNVSTAQPNSGGVSTFH
rHVR II/III	VNISSEFNAGSSSGCTVGIHGGRRVNVASSIAMTAP	FSEITVFVTHCYSSGTGSCPTGMIARDHIRISAMKN	FTFTNVSTAQPNSGGVSTFH
rHVR I/II/III	VNSTNYTSNAGSASECTVGVIKDVYNQSAASIAMTAP	FSEITVFVTHCYSSGTGSCPTGMIARDHIRISAMKN	FTFTNVSTAQPNSGGVSTFH

<sup>a</sup> Substitutions of amino acids in HVRs are shown in bold for the ck/CH/LDL/091022 strain compared with those in the Beaudette strain.

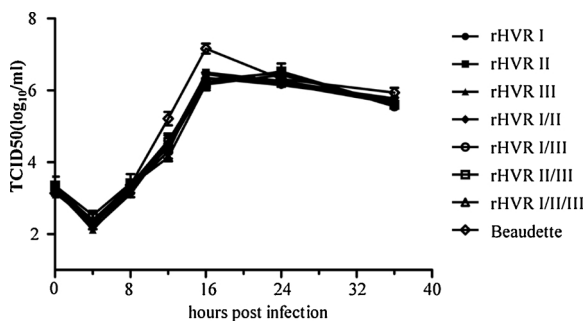


**Fig. 2.** Analysis of the growth properties of the recombinant IBVs in Vero cells. Growth curves for the recombinant IBVs in Vero cells. In order to determine the growth curves for the recombinant IBVs and Beaudette, Vero cells were infected and harvested at 0, 4, 8, 16, 24, and 36 h post-infection. Viral stocks were prepared by freezing/thawing the cells three times and TCID<sub>50</sub> was determined by infecting Vero cells in 96-well plates with 10-fold serial dilutions of each viral stock. The experiments were conducted based on three replicates. ANOVA followed Tukey’s multiple comparison tests were performed to compare the virus titers of different strains at the same time point, and differences were considered significant at  $P < 0.05$ .

**2.9. Adsorption and internalization assay using real-time RT-PCR**

Vero cells were seeded in 24-well plates (Corning) and infected with each separate strain at an MOI of 1. In the adsorption and internalization stage, total RNA was extracted from the cells, before storing at  $-80^{\circ}\text{C}$  for the subsequent quantification of viral loads, as described previously (Liu et al., 2006a; Sun et al., 2014). Three replicates were analyzed for each sample. First, the stable expression levels of three candidate reference genes comprising 18S RNA,  $\beta$ -actin, and GAPDH were compared by real-time RT-PCR in Vero cells infected with the Beaudette strain at  $4^{\circ}\text{C}$  or  $37^{\circ}\text{C}$  for 1 h. The results were analyzed using geNorm software, NormFinder software, and Delta CT (<http://150.216.56.64/referencegene.php>). The viral mRNA levels of all the samples were calculated by using the most stably expressed genes as an internal reference for normalization (Fung et al., 2014). The real-time RT-PCR results were expressed as the relative viral load adsorbed or internalized into cells relative to the Beaudette control.

**2.10. Vaccination challenge tests**

We randomly assigned 200 7-day-old SPF layer chickens to 10 groups, with 20 birds in each group. Birds in groups 1–9 were inoculated with the seven recombinant IBVs, Beaudette, and ck/CH/LDL/091022 ( $10^5 \times \text{EID}_{50}$  per bird) via intranasal and ocular routes. Birds in group 10 were inoculated with PBS and treated as the negative control. Half of the surviving birds in each group were randomly selected and challenged after 21 days with a  $10^6 \times \text{EID}_{50}$  dose of ck/CH/LDL/091022 via intranasal and ocular routes. The clinical signs were

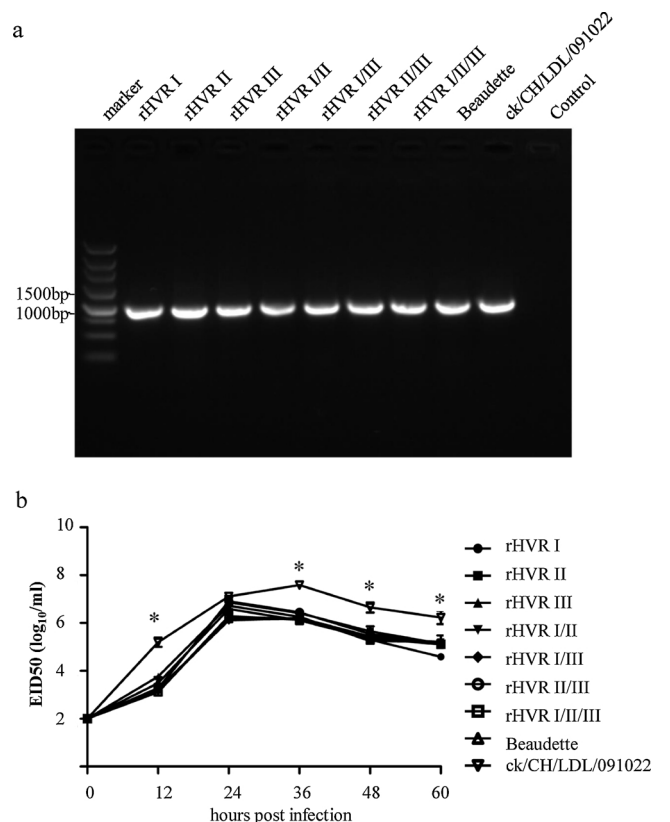


**Fig. 3.** Analysis of the growth properties of the recombinant IBVs in embryonated eggs.

(a) Detection of the recombinant IBVs in embryonated eggs. A fragment of the N gene was amplified by RT-PCR to detect the replication of the recombinant IBVs, Beaudette, and ck/CH/LDL/091022 in embryonated eggs. (b) Replication kinetics of the recombinant IBVs in embryonated eggs. The rescued IBVs and the parental strains ( $100 \times \text{EID}_{50}$ ) were inoculated into the allantoic cavities of three 9-day old embryonated eggs. The allantoic fluids from three eggs in each group were then harvested at 12, 24, 36, 48, and 60 h post-inoculation and pooled to determine the EID<sub>50</sub> values in embryonated eggs. The experiments were conducted based on three replicates. ANOVA followed Tukey’s multiple comparison tests were performed to compare the virus titers of different strains at the same time point, and differences were considered significant at  $P < 0.05$ .

monitored in the challenged birds in each group, and the morbidity and mortality rates were recorded daily. Viral shedding was also quantified using oropharyngeal swabs from the challenged chickens at 4, 8, 12, 16, and 20 days after challenge by real-time RT-PCR (Jones et al., 2011). The remaining chickens in each group were investigated for 15 days.

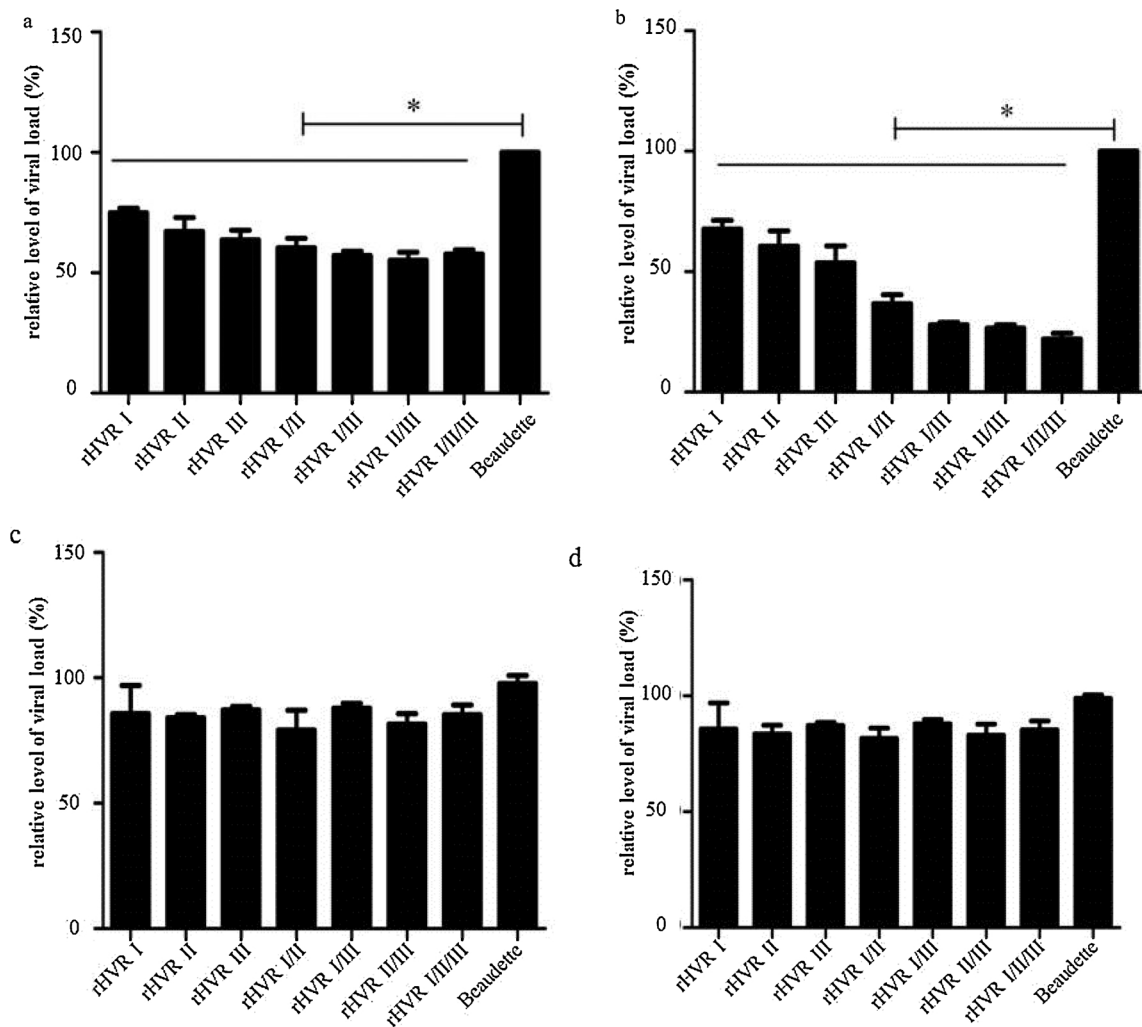


**Fig. 4.** Adsorption and internalization assays.

Vero cells were cultured in 96-well plates and infected with the recombinant IBVs and two parental strains ( $10^5 \times \text{EID}_{50}$ ) for 1 h at 4 °C or 1 h at 37 °C. The experiments were conducted based on three replicates. (a) Infected cells were fixed and cELISA was performed as described in the Materials and Methods. Results are shown as viral load adsorption on cell equivalents relative to  $\text{EID}_{50}$  compared with that in the Beaudette strain (100%). (b) Vero cells were cultured in 24-well plates and infected with the recombinant IBVs and parental strains ( $10^6 \times \text{EID}_{50}$ ) for 1 h at 4 °C. Total RNA was extracted from the infected cells before quantifying the viral loads using real-time RT-PCR. Data were normalized against the GAPDH expression levels and viral RNA was calculated relative to that in the Beaudette strain (100%). The experiments were conducted based on three replicates. (c) cELISA was performed to evaluate the viral load internalized into cells. (d) Real-time RT-PCR was also used to evaluate the viral load internalized into cells. The experiments were conducted based on three replicates. Differences were considered significant at  $P < 0.05$  using ANOVA followed Tukey's multiple comparison tests.

### 2.11. Statistical analysis

One-way ANOVA followed Tukey's multiple comparison tests were used to compare differences in the viral loads in selected tissues, as well as the results of the adsorption and internalization assays. All  $P$ -values were two-tailed and differences were considered significant when  $P < 0.05$ . In addition, Kruskal–Wallis ANOVA followed Dunn's multiple comparison tests in SPSS statistics were used to compare the trachea lesion scores and clinical scores. Differences in the survival rates were analyzed using the log-rank test.

## 3. Results

### 3.1. Rescue of the recombinant IBVs

We constructed seven full-length cDNA clones where the HVRs from Beaudette were substituted with those from ck/CH/LDL/091022 either separately or simultaneously (Fig. 1a and Table 1). The RNA transcripts generated from the full-length cDNA clones were introduced separately

into Vero cells together with the N transcripts by electroporation (Fang et al., 2005). After 48 h, the virus present in each medium was collected and used to inoculate 9-day-old SPF embryonated eggs. To differentiate the rescued viruses from the parental viruses, viral RNA was extracted from allantoic fluid and the S1 genes were amplified using RT-PCR, where the RT-PCR products covering the three HVRs were sequenced. Viral antigen was observed in Vero cells infected with the Beaudette strain and the seven recombinant IBVs (Fig. 1b). No virus antigen was found in cells infected with ck/CH/LDL/091022. RT-PCR analysis of subgenomic mRNA 3 and mRNA 4 was performed to confirm the virus replication (Fig. 1c) (Fang et al., 2007). The results confirmed that the recombinant IBVs were adapted to Vero cells in a similar manner to the Beaudette strain.

### 3.2. Characterization of the rescued IBVs

To test whether exchanging the HVRs affected the growth properties and genetic stability of the rescued viruses, the recombinant IBVs were propagated on embryonated eggs or Vero cells for three passages. The

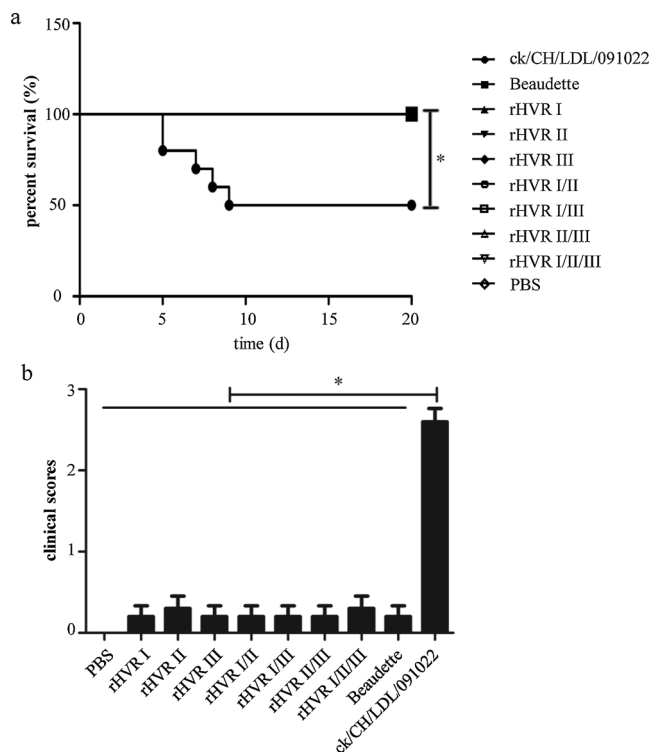


Fig. 5. Pathogenicity test.

(a) Mortality was recorded daily for 10 randomly selected infected birds and the survival curve was drawn. (b) At 5 days after challenge, we evaluated the challenged chickens blindly and clinical signs were scored as: 0 = absent, 1 = mild, 2 = moderate, or 3 = severe. Kruskal–Wallis ANOVA followed Dunn's multiple comparison tests were employed to perform comparisons of the clinical scores using SPSS.

S1 gene sequencing results confirmed that the heterogenous HVRs were stably maintained in the recombinant IBVs (Sup Fig. 1), and no additional mutations were detected in the S protein after three passages in cells or eggs. The growth properties of the recombinant IBVs were then determined in Vero cells and embryonated eggs. In Vero cells (Fig. 1c), the growth kinetics of the recombinant IBVs were similar to those of the Beaudette strain, and they all reached their peak titer at 16 h post-infection, and there was no significant difference between the titers for the recombinant IBVs and Beaudette at different time points (Fig. 2). In embryonated eggs (Fig. 3a), although there were no significant difference between the virus titers for the recombinant IBVs and Beaudette at different time points, the titers of ck/CH/LDL/091022 was significantly higher than those of the recombinant IBVs and Beaudette at 12, 36, 48, 60 h (Fig. 3b). In conclusion, the recombinant IBVs exhibited similar growth phenotypes compared to the Beaudette strain in both cells and eggs.

### 3.3. Adsorption and internalization assays

The IF staining results showed the IBV N antigens in Vero cells infected with the recombinant IBVs (Fig. 1b) and they have the similar ability to replicate in Vero cells with IBV Beaudette. We then evaluated the effects of the heterogenous HVRs on virus adsorption and internalization. The cELISA results for the adsorption assay showed that compared with Beaudette, the recombinant IBVs exhibited significantly reduced adsorption at 4 °C for 1 h (Fig. 4a). The real-time RT-PCR results were consistent with the cELISA results in the adsorption assays (Fig. 4b). The results indicated that the heterogenous HVRs could reduce the adsorption capacity of the recombinant IBVs. In addition, the cELISA results from the internalization assay showed that the viral yields of the recombinant IBVs internalized into cells did not differ

significantly from those with Beaudette (Fig. 4c). The real-time RT-PCR results were consistent with the cELISA results from the internalization assay (Fig. 4d).

### 3.4. Pathogenicity of the recombinant IBVs

In order to test the pathogenicity of the recombinant IBVs, 7-day-old SPF chickens were inoculated via intranasal and ocular routes at a dose of  $10^5 \times \text{EID}_{50}$  per bird (Sun et al., 2011). We found that some of the chickens only had very low levels of snicking at 6 and 7 days post-infection, and there were no obvious clinical signs in the groups treated with the recombinant IBVs and Beaudette. However, 5/10 birds (50%) died during 5–9 days post-challenge with ck/CH/LDL/091022 and the morbidity rate was 100% (Fig. 5a). The mean scores for the clinical signs in the birds inoculated with the recombinant IBVs and Beaudette were much lower than those treated with ck/CH/LDL/091022 (Fig. 5b). The autopsy results showed that ck/CH/LDL/091022 caused obvious swollen pale kidneys, where the tubules and ureters were distended with urates, thereby indicating the nephropathogenic potential of the virus. However, the autopsies detected almost no changes in the groups treated with the recombinant IBVs and Beaudette. The H&E staining results also showed that there were no obvious pathological change in the lungs, cecum tonsils, and kidneys in the groups treated with the recombinant IBVs and Beaudette (Sup Fig. 2). We also assessed the severity scores for histopathological lesions in the trachea with deciliation (Fig. 6a), goblet cells (Fig. 6b), mucosal thickness (Fig. 6c), and lymphocytes (Fig. 6d) at 5 days after challenge with the IBVs (van Ginkel et al., 2015). The scores were lowest in the Beaudette group and highest in the ck/CH/LDL/091022 group, and there were no differences in the scores between the groups treated with the recombinant IBVs and Beaudette. However, the scores in the groups treated with the recombinant IBVs and Beaudette differed significantly from those with ck/CH/LDL/091022. Finally, no IBV RNA was detected in the oropharyngeal swabs from chickens inoculated with the recombinant IBVs and Beaudette after 4, 8, 12, 16, and 20 days by real-time RT-PCR, where the results were considered positive when the Ct value was less than 32 (Li et al., 2016; Zhao et al., 2017). The results confirmed that the recombinant IBVs were avirulent according to the histomorphometry and histopathology findings.

### 3.5. Serotypes of the recombinant IBVs

Using a previously described method (Archetti and Horsfall et al., 1950), the serotype relatedness values were calculated based on the cross-virus neutralization studies using Vero cells (Table 2) or embryonated chicken eggs (Table 3). Viruses with an Archetti and Horsfall relatedness value greater than 25 were considered to be related serotypes. Our results showed that the recombinant IBVs and Beaudette belonged to the same serotype (Table 2), whereas the recombinant IBVs and ck/CH/LDL/091022 belonged to different serotypes (Table 3). In general, we found that the serotype relatedness values decreased between the recombinant strain and Beaudette (Table 2) as the number of substituted heterogenous HVRs increased. These results confirmed that the replacement of the heterogenous HVRs had not caused serotype switches in this case.

### 3.6. In vivo tissue tropisms

The IHC results showed that the viral antigen of ck/CH/LDL/091022 was detected in trachea (Sup Fig. 3a), cecal tonsil (Sup Fig. 3b), and kidney samples (Sup Fig. 3c), but the results were negative in the tissues infected with the recombinant IBVs and Beaudette. The results were also negative in all of the lung samples (Sup Fig. 3d). The viral RNA could be detected by real-time RT-PCR in the selected tissues from chickens infected with ck/CH/LDL/091022, with high viral loads in the kidneys. However, very low RNA levels were detected in only a few

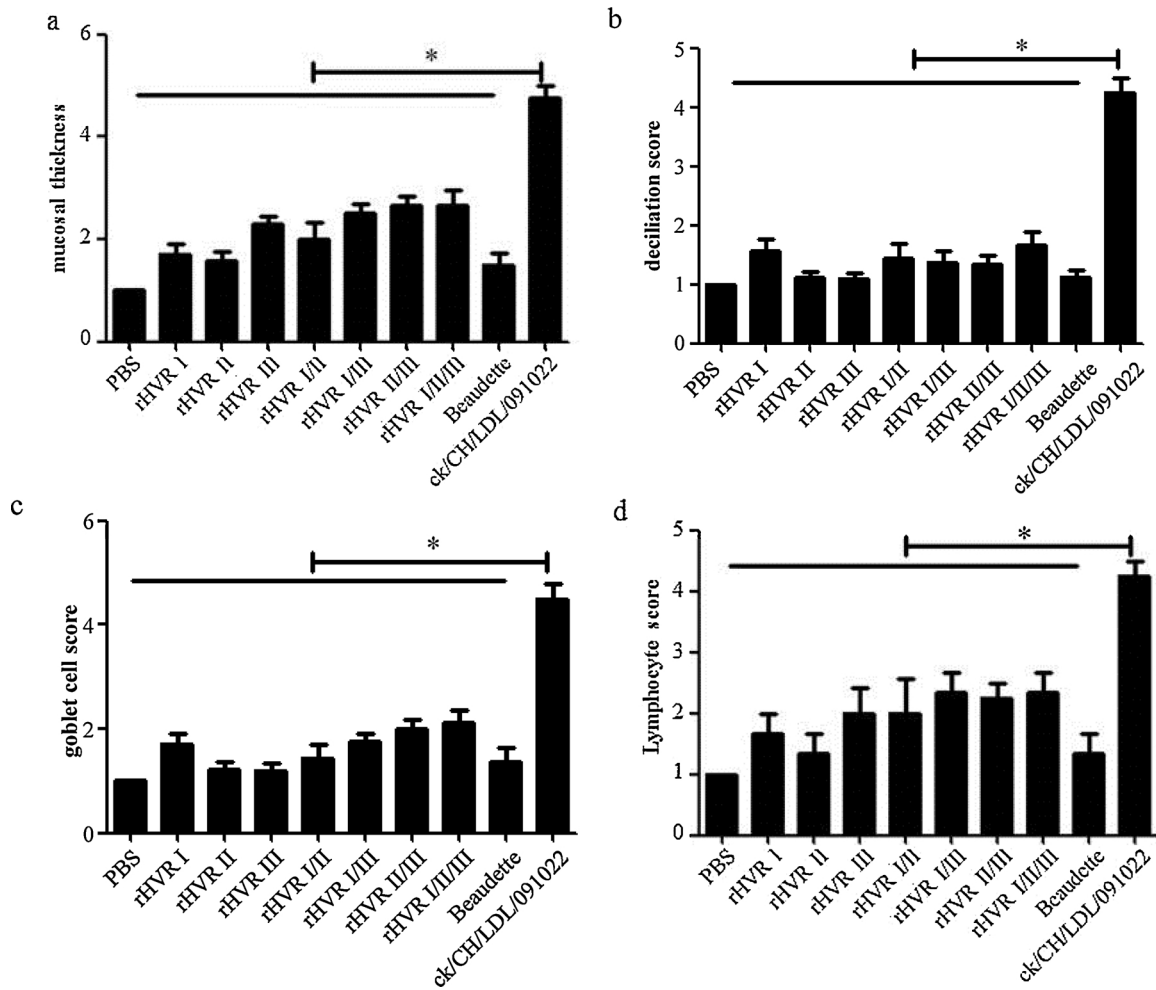


Fig. 6. Trachea lesion scores.

At 5 days after challenge, the other five infected birds in each group were killed humanely using carbon dioxide over inhalation. Tissue samples were collected from the trachea and analyzed by H&E staining. Mucosal thickness (a), deciliation (b), goblet cells (c) and lymphocyte scores (d) for the trachea samples were evaluated blindly and scored from 1 to 5 based on severity. Kruskal–Wallis and Dunn–Bonferroni tests were employed to perform post hoc comparisons of trachea lesion scores using SPSS.

Table 2

Results of neutralization tests using the recombinant IBVs and Beaudette strains in Vero cells (%).

	1	2	3	4	5	6	7	8
1. rHVR I	100							
2. rHVR II	54.9	100						
3. rHVR III	56.4	66.6	100					
4. rHVR I/II	64.1	72.1	65.5	100				
5. rHVR I/III	73.8	45.0	69.6	44.2	100			
6. rHVR II/III	42.3	45.8	67.1	45.0	49.4	100		
7. rHVR I/II/III	40.2	44.1	52.6	43.1	46.7	65.9	100	

Virus replication was found in Vero cells infected with Beaudette and the recombinant IBVs, so the neutralization tests between them were performed in Vero cells.

Table 3

Results of neutralization tests using the recombinant IBVs and two parental strains in embryonated eggs (%).

	rHVR I	rHVR II	rHVR III	rHVR I/II	rHVR I/III	rHVR II/III	rHVR I/II/III	Beaudette
ck/CH/LDL/091022	< 2	< 2	< 2	< 2	< 2	< 2	< 2	< 2

ck/CH/LDL/091022 could not produce CPE in Vero cells so the neutralization tests between ck/CH/LDL/091022 and other strains were performed in embryonated eggs.

trachea samples from the birds infected with the recombinant IBVs and Beaudette (Fig. 7). These results confirmed that the recombinant IBVs had the same tissue tropism as the Beaudette strain.

### 3.7. Vaccination challenge tests

Inoculating chickens with the seven recombinant IBVs induced clinical protection against challenge with ck/CH/LDL/091022 (Table 4). Viral shedding was detected in some of the chickens challenged with ck/CH/LDL/091022, but inoculating chickens with the seven recombinant IBVs and Beaudette reduced the morbidity and mortality rates compared with birds in the PBS group. However, the morbidity and mortality of the recombinant IBVs and Beaudette vaccinated groups was not as low as that of ck/CH/LDL/091022 inoculated group. These results suggest that although the recombinant IBVs could

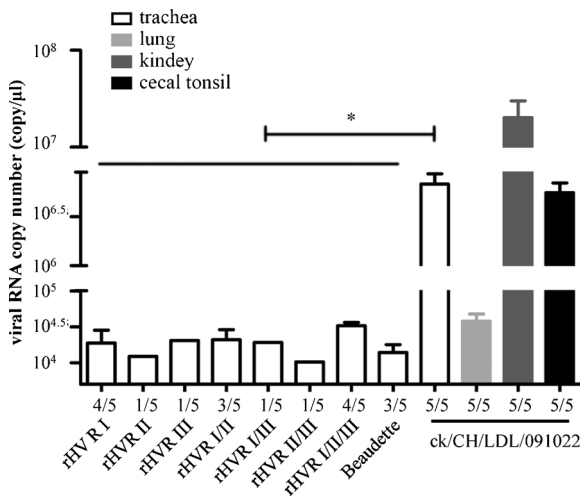


**Fig. 7.** Detection of IBV replication in challenged chickens. At 5 days after challenge, the other five infected birds in each group were killed humanely using carbon dioxide over inhalation, and tissue samples of the trachea, lungs, kidneys, and cecum tonsils were collected to determine the presence of IBV by real-time RT-PCR. A Ct value less than 32 was considered to be IBV-positive using real-time RT-PCR. The numbers of tissue samples positive for IBV RNA/the number detected are presented at the bottom. Bars in different colors represent different tissues from chickens, as indicated in the graphical representation. The average copy numbers of IBV RNA in the positive samples are shown. Differences were considered significant at  $P < 0.05$  using ANOVA followed Tukey's multiple comparison tests.

not offer complete protection against challenge with ck/CH/LDL/091022, inoculation with the seven recombinant IBVs did confer some cross protection against ck/CH/LDL/091022 challenge.

**4. Discussion**

Coronavirus IBV S protein has multiple biological functions during the viral replication cycle. Previous studies suggest that some of these functions may be associated with HVRs in the S1 subunit of the S protein (Cavanagh and Davis, 1986; Ignjatovic and Galli, 1994; Johnson et al., 2003; Song et al., 1998). These previous studies employed forward genetics methods to determine the effects of the HVRs on serotypes by characterizing phylogenetically closely related isolates. However, these strains inevitably had mutations in other parts of the IBV genome, thereby making it difficult to establish a precise model for further studies based on these previous findings. In the present study,

we manipulated the IBV RNA genomes by reverse genetics to produce site-directed mutations in order to elucidate the specific biological functions of the HVRs.

We used the Beaudette and ck/CH/LDL/091022 strains in our study. IBV Beaudette is a well-known apathogenic lab strain (Geilhausen et al., 1973), which was adapted to Vero cells from chicken embryos (Fang et al., 2005). The ck/CH/LDL/091022 IBV strain is an epidemic strain isolated from H120-vaccinated layers in China. This strain mainly causes gross lesions in chicken kidneys, with high morbidity and mortality rates (Liu et al., 2008, 2009; Liu et al., 2006b). The ck/CH/LDL/091022 strain can only proliferate in chicken embryos and not Vero cells. In addition, the Beaudette and ck/CH/LDL/091022 strains belong to different serotypes. Thus, the differences in these two strains facilitate research into the effects of the HVRs in intact viral particles on serotypes, virulence, and tropisms.

In order to determine the roles of individual HVRs and the accumulated effects of HVRs, we constructed seven recombinant IBVs where the three HVRs in the Beaudette strain were separately or simultaneously substituted with those from ck/CH/LDL/091022. All of the recombinant IBVs proliferated in Vero cells (Figs. 1b and Figure 2), and had the similar growth kinetics as Beaudette in Vero cells (Fig. 2) and embryonated eggs (Fig. 3b). The accumulation of heterogenous HVRs weakened the capacity for adsorption during infection by the recombinant viruses *in vitro* (Fig. 4a and b). The HVRs may be associated with the receptor-binding domain, so the heterogenous HVRs weakened the interaction between the viruses and their receptors on the host cells. With the same sequences of fusion subunit S2, the recombinant IBVs and Beaudette did not differ significantly in the internalization assay. It is unclear whether the recombinant viruses have more efficient internalization than Beaudette and the S proteins assemble correctly in the recombinant viruses, and whether there is a comparable amount of S on the virus particle. These problems require for further investigation.

Both the recombinant IBVs and Beaudette only weakly infected the trachea in 7-day-old SPF chickens (Fig. 5e), whereas ck/CH/LDL/091022 infected multiple chicken tissues, including the trachea, lungs, kidneys, and cecal tonsils. Thus, the replication capacity was similar for the recombinant IBVs and the Beaudette strain in SPF chickens. It appears that only swapping the HVRs did not greatly affect the cell and tissue tropisms, although replacing the ectodomain of the S glycoprotein in the Beaudette strain can alter the growth characteristics (Casais et al., 2003). Virus binding to host cells is the first step in tropism determination and HVRs within the S1 subunit may affect IBV binding (Wickramasinghe et al., 2011), but S2 is responsible for membrane fusion (Sun et al., 2017), and thus exchanging the HVRs did not change their tropism.

**Table 4**  
Results of vaccination challenge tests.

Group	Morbidity	Mortality	Virus recovery <sup>a</sup>					Antibody response									
								Vaccinated					Challenged				
			4d <sup>b</sup>	8d	12d	16d	20d	4d	8d	12d	16d	20d	4d	8d	12d	16d	20d
rHVR I	7/10	1/10	10/10	4/9	2/9	1/9	0/9	0/10	2/10	3/10	7/10	10/10	6/10	9/9	9/9	9/9	9/9
rHVR II	7/10	1/10	10/10	7/9	4/9	2/9	0/9	0/10	1/10	3/10	5/10	10/10	7/10	9/9	9/9	9/9	9/9
rHVR III	8/10	1/10	10/10	5/9	2/9	1/9	0/9	0/10	2/10	4/10	5/10	10/10	6/10	9/9	9/9	9/9	9/9
rHVR I/II	7/10	0/10	10/10	6/10	4/10	0/10	0/10	0/10	3/10	5/10	7/10	10/10	7/10	10/10	10/10	10/10	10/10
rHVR I/III	7/10	1/10	10/10	7/9	2/9	0/9	0/9	0/10	2/10	4/10	6/10	10/10	6/10	9/9	9/9	9/9	9/9
rHVR II/III	8/10	2/10	10/10	6/8	1/8	0/8	0/8	0/10	1/10	3/10	6/10	10/10	7/10	8/8	8/8	8/8	8/8
rHVR I/II/III	7/10	0/10	10/10	6/10	5/10	0/10	0/10	0/10	2/10	5/10	7/10	10/10	8/10	10/10	10/10	10/10	10/10
Beaudette	9/10	1/10	10/10	4/9	4/9	1/9	0/9	0/10	2/10	4/10	6/10	10/10	6/10	9/9	9/9	9/9	9/9
ck/CH/LDL/091022	2/5 <sup>c</sup>	0/5	5/5	3/5	2/5	0/5	0/5	0/10	5/6	5/5	5/5	5/5	5/5	5/5	5/5	5/5	5/5
PBS	10/10	3/10	10/10	8/9	3/7	0/7	0/7	0/10	0/10	0/10	0/10	0/10	3/10	4/9	5/7	7/7	7/7

<sup>a</sup> Viral RNA was detected in oral swab samples by real-time RT-PCR and samples with a Ct value less than 32 were considered positive.

<sup>b</sup> Days after challenge.

<sup>c</sup> Five birds died 7 days after inoculation with ck/CH/LDL/091022.

Previous studies have shown that the S protein has major effects on pathogenicity in coronaviruses (Leparc-Goffart et al., 1997; Phillips et al., 2001), but the specific effects of HVRs in the S protein on pathogenicity are not clear. In the present study, the recombinant IBVs remained avirulent with the HVRs from pathogenic ck/CH/LDL/091022, thereby indicating that only exchanging the HVR sequences did not have major impacts on pathogenicity (Figs. 5 and 6, Sup. Fig. 2). According to Hodgson et al., the apathogenic nature of the recombinant IBV BeauR-M41(S) indicates that the S protein ectodomain from a virulent strain is not necessarily sufficient to overcome the attenuating mutations in other genes in the apathogenic Beaudette strain (Hodgson et al., 2004). It is possible that the replicase gene also contributes to the pathogenicity of IBV (Armesto et al., 2009; Hodgson et al., 2004). The functions of non-structural proteins (Nsp) in the context of pathogenesis are still not well understood, but some of the Nsps in other coronaviruses have been linked to loss of pathogenicity (Eriksson et al., 2008; Sperry et al., 2005).

It is considered that the HVRs of the IBV S1 subunit may induce abundant virus neutralizing antibodies (Kant et al., 1992; Koch et al., 1990; Moore et al., 1997; Niesters et al., 1987). However, in our study, the introduction of heterogenous HVRs did not develop an independent serotype, although the antigenic relatedness values for the recombinant IBVs and Beaudette generally decreased as the number of heterogenous HVR exchanges increased (Table 2). This result is consistent with the conclusion of Santos Fernando et al. who found that three IBV isolates mainly exhibited mutations in the HVRs but they belonged to the same serotype (Santos Fernando et al., 2017). The repertoire of neutralizing polyclonal antibodies may react with the many epitopes of an antigen. Exchanging the HVRs could change several antigen determinants but it is not necessarily sufficient to change the serotype because other neutralizing epitopes have been identified in other parts of the S1 subunit and S2 subunit (Ignjatovic and Sapats, 2005; Kusters et al., 1989; Lenstra et al., 1989). In particular cases, a very low number of critical amino acid changes is sufficient to greatly alter the antigenicity (Cavanagh et al., 1992), although this view does not apply in all cases (Chen et al., 2015). In conclusion, the recombinant IBVs exhibited differences in antigenicity, but exchanging only the three HVRs between the two parental strains did not change the serotype.

Vaccination is considered the most cost-effective approach for controlling IBV infection. However, current commercial vaccines have been challenged by the emergence of new IBV serotypes. Recently, reverse genetic techniques have been employed to modify IBV vaccine candidates. QX-like strains (LX4-type) emerged in China and spread to Asia (Mahmood et al., 2011), Russia (Bochkov et al., 2006), and Europe (Beato et al., 2005; Worthington et al., 2008). In this study, using ck/CH/LDL/091022 as a representative of epidemic QX-like strains, we modified the genome of the Beaudette strain to construct seven recombinant IBVs. We determined the effects of the HVRs and explored the possibility of developing a vaccine candidate that could proliferate in cells and provide protection against the prevalent field strains. The introduction of a few heterogenous peptides rather than the whole S protein may facilitate the development of multi-epitope peptide vaccines to protect against a wide range of IBV serotypes (Yang et al., 2009). In the present study, the virus cross-neutralization and vaccination challenge tests indicated that only swapping the HVRs did not provide sufficient cross-protection, but further exploration of the recombinant IBVs may provide insights into novel vaccine candidates.

In conclusion, we manipulated the genome of the IBV Beaudette strain using a reverse genetics system to construct seven recombinant strains by replacing the HVRs in the Beaudette strain with the corresponding fragments from a QX-like nephropathogenic isolate ck/CH/LDL/091022 from China. The results showed that the heterogenous HVRs could weaken the capacity for adsorption during infection *in vitro*, as well as reducing the antigenic relatedness values between the recombinant strains and Beaudette. The results obtained in this study help to understand the prevention and control of IBV.

## Conflict of interest

All authors declare that they have no conflict of interest.

## Acknowledgments

This work was supported by grants from the China Agriculture Research System (No. CARS-41-K18), the Provincial Supported Science Foundation of Heilongjiang Province for The National Key Technology R&D Program (GX16B003) and National "Twelfth Five-Year" Plan for Science & Technology Support (2015BAD12B03). The authors declare that they have no competing interests.

## Appendix A. Supplementary data

Supplementary material related to this article can be found, in the online version, at doi:<https://doi.org/10.1016/j.virusres.2018.04.013>.

## References

- Archetti, I., Horsfall Jr., F.L., 1950. Persistent antigenic variation of influenza A viruses after incomplete neutralization in ovo with heterologous immune serum. *J. Exp. Med.* 92 (5), 441–462.
- Armesto, M., Cavanagh, D., Britton, P., 2009. The replicase gene of avian coronavirus infectious bronchitis virus is a determinant of pathogenicity. *PLoS One* 4 (10), e7384.
- Beato, M.S., De Battisti, C., Terregino, C., Drago, A., Capua, I., Ortali, G., 2005. Evidence of circulation of a Chinese strain of infectious bronchitis virus (QXIBV) in Italy. *Vet. Rec.* 156 (May (22)), 720.
- Bochkov, Y.A., Batchenko, G.V., Shcherbakova, L.O., Borisov, A.V., Drygin, V.V., 2006. Molecular epizootiology of avian infectious bronchitis in Russia. *Avian Pathol.* 35 (5), 379–393.
- Casais, R., Dove, B., Cavanagh, D., Britton, P., 2003. Recombinant avian infectious bronchitis virus expressing a heterologous spike gene demonstrates that the spike protein is a determinant of cell tropism. *J. Virol.* 77 (16), 9084–9089.
- Cavanagh, D., 2003. Severe acute respiratory syndrome vaccine development: experiences of vaccination against avian infectious bronchitis coronavirus. *Avian Pathol.* 32 (6), 567–582.
- Cavanagh, D., Davis, P.J., 1986. Coronavirus IBV: removal of spike glycoprotein by urea abolishes infectivity and haemagglutination but not attachment to cells. *J. Gen. Virol.* 67 (7), 1443–1448.
- Cavanagh, D., Davis, P.J., Mockett, A.P., 1988. Amino acids within hypervariable region 1 of avian coronavirus IBV (Massachusetts serotype) spike glycoprotein are associated with neutralization epitopes. *Virus Res.* 11 (2), 141–150.
- Cavanagh, D., Davis, P.J., Cook, J.K., Li, D., Kant, A., Koch, G., 1992. Location of the amino acid differences in the S1 spike glycoprotein subunit of closely related serotypes of infectious bronchitis virus. *Avian Pathol.* 21 (1), 33–43.
- Chen, L., Zhang, T., Han, Z., Liang, S., Xu, Y., Xu, Q., Chen, Y., Zhao, Y., Shao, Y., Li, H., Wang, K., Kong, X., Liu, S., 2015. Molecular and antigenic characteristics of Massachusetts genotype infectious bronchitis coronavirus in China. *Vet. Microbiol.* 181 (3), 241–251.
- de Groot, R.J., Luytjes, W., Horzinek, M.C., van der Zeijst, B.A., Spaan, W.J., Lenstra, J.A., 1987. Evidence for a coiled-coil structure in the spike proteins of coronaviruses. *J. Mol. Biol.* 196 (4), 963–966.
- de Wit, J.J., Nieuwenhuisen-van Wilgen, J., Hoogkamer, A., van de Sande, H., Zuidam, G.J., Fabri, T.H., 2011. Induction of cystic oviducts and protection against early challenge with infectious bronchitis virus serotype D388 (genotype QX) by maternally derived antibodies and by early vaccination. *Avian Pathol.* 40 (5), 463–471.
- Eriksson, K.K., Cervantes-Barragan, L., Ludewig, B., Thiel, V., 2008. Mouse hepatitis virus liver pathology is dependent on ADP-ribose-10phosphatase, a viral function conserved in the alpha-like supergroup. *J. Virol.* 82 (24), 12325–12334.
- Fang, S.G., Shen, S., Tay, F.P., Liu, D.X., 2005. Selection of and recombination between minor variants lead to the adaptation of an avian coronavirus to primate cells. *Biochem. Biophys. Res. Commun.* 336 (2), 417–423.
- Fang, S., Chen, B., Tay, F.P., Ng, B.S., Liu, D.X., 2007. An arginine-to-proline mutation in a domain with undefined functions within the helicase protein (Nsp13) is lethal to the coronavirus infectious bronchitis virus in cultured cells. *Virology* 358 (1), 136–147.
- Fang, S., Shen, H., Wang, J., Tay, F.P., Liu, D.X., 2010. Functional and genetic studies of the substrate specificity of coronavirus infectious bronchitis virus 3C-like proteinase. *J. Virol.* 84 (14), 7325–7336.
- Fung, T.S., Huang, M., Liu, D.X., 2014. Coronavirus-induced ER stress response and its involvement in regulation of coronavirus-host interactions. *Virus Res.* 194 (1), 110–123.
- Geilhausen, H.E., Ligon, F.B., Lukert, P.D., 1973. The pathogenesis of virulent and avirulent avian infectious bronchitis virus. *Arch. Gesamte Virusforsch.* 40 (3), 285–290.
- Han, Z., Zhao, F., Shao, Y., Liu, X., Kong, X., Song, Y., Liu, S., 2013. Fine level epitope mapping and conservation analysis of two novel linear B-cell epitopes of the avian infectious bronchitis coronavirus nucleocapsid protein. *Virus Res.* 171 (1), 54–64.
- Hodgson, T., Casais, R., Dove, B., Britton, P., Cavanagh, D., 2004. Recombinant infectious bronchitis coronavirus beaudette with the spike protein gene of the pathogenic M41

- strain remains attenuated but induces protective immunity. *J. Virol.* 78 (24), 13804–13811.
- Ignjatovic, J., Galli, L., 1994. The S1 glycoprotein but not the N or M proteins of avian infectious bronchitis virus induces protection in vaccinated chickens. *Arch. Virol.* 138 (1–2), 117–134.
- Ignjatovic, J., Sapats, S., 2005. Identification of previously unknown antigenic epitopes on the S and N proteins of avian infectious bronchitis virus. *Arch. Virol.* 150 (9), 1813–1831.
- Johnson, M.A., Pooley, C., Ignjatovic, J., Tyack, S.G., 2003. A recombinant fowl adenovirus expressing the S1 gene of infectious bronchitis virus protects against challenge with infectious bronchitis virus. *Vaccine* 21 (21–22), 2730–2736.
- Jones, R.M., Ellis, R.J., Cox, W.J., Errington, J., Fuller, C., Irvine, R.M., Wakeley, P.R., 2011. Development and validation of RT-PCR tests for the detection and S1 genotyping of infectious bronchitis virus and other closely related gammacoronaviruses within clinical samples. *Transbound. Emerg. Dis.* 58 (5), 411–420.
- Kant, A., Koch, G., van Roozelaar, D.J., Kusters, J.G., Poelwijk, F.A., van der Zeijst, B.A., 1992. Location of antigenic sites defined by neutralizing monoclonal antibodies on the S1 avian infectious bronchitis virus glycopolyptide. *J. Gen. Virol.* 73 (3), 591–596.
- Koch, G., Hartog, L., Kant, A., van Roozelaar, D.J., 1990. Antigenic domains on the peplomer protein of avian infectious bronchitis virus: correlation with biological functions. *J. Gen. Virol.* 71 (9), 1929–1935.
- Kusters, J.G., Jager, E.J., Lenstra, J.A., Koch, G., Posthumus, W.P., Meloen, R.H., van der Zeijst, B.A., 1989. Analysis of an immunodominant region of infectious bronchitis virus. *J. Immunol.* 143 (8), 2692–2698.
- Lenstra, J.A., Kusters, J.G., Koch, G., van der Zeijst, B.A., 1989. Antigenicity of the peplomer protein of infectious bronchitis virus. *Mol. Immunol.* 26 (1), 7–15.
- Leparc-Goffart, I., Hingley, S.T., Chua, M.M., Jiang, X., Lavi, E., Weiss, S.R., 1997. Altered pathogenesis of a mutant of the murine coronavirus MHV-A59 is associated with a Q159L amino acid substitution in the spike protein. *Virology* 239 (1), 1–10.
- Li, H., Wang, Y., Han, Z., Liang, S., Jiang, L., Hu, Y., Kong, X., Liu, S., 2016. Recombinant duck enteritis viruses expressing major structural proteins of the infectious bronchitis virus provide protection against infectious bronchitis in chickens. *Antivir. Res.* 130, 19–26.
- Liu, D.X., Brierley, I., Brown, T.D., 1995. Identification of a trypsin-like serine proteinase domain encoded by ORF 1a of the coronavirus IBV. *Adv. Exp. Med. Biol.* 380 (3), 405–411.
- Liu, D.X., Shen, S., Xu, H.Y., Wang, S.F., 1998. Proteolytic mapping of the coronavirus infectious bronchitis virus 1b polyprotein: evidence for the presence of four cleavage sites of the 3C-like proteinase and identification of two novel cleavage products. *Virology* 246 (2), 288–297.
- Liu, S., Chen, J., Han, Z., Zhang, Q., Shao, Y., Kong, X., Tong, G., 2006a. Infectious bronchitis virus: S1 gene characteristics of vaccines used in China and efficacy of vaccination against heterologous strains from China. *Avian Pathol.* 35 (5), 394–399.
- Liu, S.W., Zhang, Q.X., Chen, J.D., Han, Z.X., Liu, X., Feng, L., Shao, Y.H., Rong, J.G., Kong, X.G., Tong, G.Z., 2006b. Genetic diversity of avian infectious bronchitis coronavirus strains isolated in China between 1995 and 2004. *Arch. Virol.* 151 (6), 1133–1148.
- Liu, S., Wang, Y., Ma, Y., Han, Z., Zhang, Q., Shao, Y., Chen, J., Kong, X., 2008. Identification of a newly isolated avian infectious bronchitis coronavirus variant in China exhibiting affinity for the respiratory tract. *Avian Dis.* 52 (2), 306–314.
- Liu, S., Zhang, X., Wang, Y., Li, C., Han, Z., Shao, Y., Li, H., Kong, X., 2009. Molecular characterization and pathogenicity of infectious bronchitis coronaviruses: complicated evolution and epidemiology in China caused by cocirculation of multiple types of infectious bronchitis coronaviruses. *Intervirology* 52 (4), 223–234.
- Liu, X., Ma, H., Xu, Q., Sun, N., Han, Z., Sun, C., Guo, H., Shao, Y., Kong, X., Liu, S., 2013. Characterization of a recombinant coronavirus infectious bronchitis virus with distinct S1 subunits of spike and nucleocapsid genes and a 3' untranslated region. *Vet. Microbiol.* 162 (2), 429–436.
- Mahmood, Z.H., Sleman, R.R., Uthman, A.U., 2011. Isolation and molecular characterization of Sul/01/09 avian infectious bronchitis virus, indicates the emergence of a new genotype in the Middle East. *Vet. Microbiol.* 150 (1–2), 21–227.
- Moore, K.M., Jackwood, M.W., Hilt, D.A., 1997. Identification of amino acids involved in a serotype and neutralization specific epitope within the s1 subunit of avian infectious bronchitis virus. *Arch. Virol.* 142 (11), 2249–2256.
- Niester, H.G., Bleumink-Pluym, N.M., Osterhaus, A.D., Horzinek, M.C., van der Zeijst, B.A., 1987. Epitopes on the peplomer protein of infectious bronchitis virus strain M41 as defined by monoclonal antibodies. *Virology* 161 (2), 511–519.
- Phillips, J.J., Chua, M., Seo, S.H., Weiss, S.R., 2001. Multiple regions of the murine coronavirus spike glycoprotein influence neurovirulence. *J. Neurovirol.* 7 (5), 421–431.
- Promkuntod, N., van Eijndhoven, R.E., de Vrieze, G., Grone, A., Verheije, M.H., 2014. Mapping of the receptor-binding domain and amino acids critical for attachment in the spike protein of avian coronavirus infectious bronchitis virus. *Virology* 448 (2), 26–32.
- Santos Fernando, F., Coelho Kasmanas, T., Diniz Lopes, P., da Silva Montassier, M.F., Zanella Mores, M.A., Casagrande Mariguela, V., Pavani, C., Moreira Dos Santos, R., Assayag Jr., M.S., Montassier, H.J., 2017. Assessment of molecular and genetic evolution, antigenicity and virulence properties during the persistence of the infectious bronchitis virus in broiler breeders. *J. Gen. Virol.* 98 (10), 2470–2481.
- Shil, P.K., Kanci, A., Browning, G.F., Markham, P.F., 2011. Development and immunogenicity of recombinant GapA(+) *Mycoplasma gallisepticum* vaccine strain ts-11 expressing infectious bronchitis virus-S1 glycoprotein and chicken interleukin-6. *Vaccine* 29 (17), 3197–3205.
- Song, C.S., Lee, Y.J., Lee, C.W., Sung, H.W., Kim, J.H., Mo, I.P., Izumiya, Y., Jang, H.K., Mikami, T., 1998. Induction of protective immunity in chickens vaccinated with infectious bronchitis virus S1 glycoprotein expressed by a recombinant baculovirus. *J. Gen. Virol.* 79 (4), 719–723.
- Sperry, S.M., Kazi, L., Graham, R.L., Baric, R.S., Weiss, S.R., Denison, M.R., 2005. Single amino-acid substitutions in open reading frame (ORF) 1b-nsP14 and ORF 2a proteins of the coronavirus mouse hepatitis virus are attenuating in mice. *J. Virol.* 79 (6), 3391–3400.
- Sun, C., Han, Z., Ma, H., Zhang, Q., Yan, B., Shao, Y., Xu, J., Kong, X., Liu, S., 2011. Phylogenetic analysis of infectious bronchitis coronaviruses newly isolated in China, and pathogenicity and evaluation of protection induced by Massachusetts serotype H120 vaccine against QX-like strains. *Avian Pathol.* 40 (1), 43–54.
- Sun, J., Han, Z., Shao, Y., Cao, Z., Kong, X., Liu, S., 2014. Comparative proteome analysis of tracheal tissues in response to infectious bronchitis coronavirus, Newcastle disease virus, and avian influenza virus H9 subtype virus infection. *Proteomics* 14 (11), 1403–1423.
- Sun, J., Han, Z., Qi, T., Zhao, R., Liu, S., 2017. Chicken galectin-1B inhibits Newcastle disease virus adsorption and replication through binding to hemagglutinin-neuraminidase (HN) glycoprotein. *J. Biol. Chem.* 292 (49), 20141–20161.
- Tan, Y.W., Fang, S., Fan, H., Lescar, J., Liu, D.X., 2006. Amino acid residues critical for RNA-binding in the N-terminal domain of the nucleocapsid protein are essential determinants for the infectivity of coronavirus in cultured cells. *Nucleic Acids Res.* 34 (17), 4816–4825.
- Tay, F.P., Huang, M., Wang, L., Yamada, Y., Liu, D.X., 2012. Characterization of cellular furin content as a potential factor determining the susceptibility of cultured human and animal cells to coronavirus infectious bronchitis virus infection. *Virology* 433 (2), 421–430.
- van Ginkel, F.W., Padgett, J., Martinez-Romero, G., Miller, M.S., Joiner, K.S., Gulley, S.L., 2015. Age-dependent immune responses and immune protection after avian coronavirus vaccination. *Vaccine* 33 (23), 2655–2661.
- Wadey, C.N., Faragher, J.T., 1981. Australian infectious bronchitis viruses: identification of nine subtypes by a neutralisation test. *Res. Vet. Sci.* 30 (1), 70–74.
- Wickramasinghe, I.N., de Vries, R.P., Grone, A., de Haan, C.A., Verheije, M.H., 2011. Binding of avian coronavirus spike proteins to host factors reflects virus tropism and pathogenicity. *J. Virol.* 85 (17), 8903–8912.
- Worthington, K.J., Currie, R.J., Jones, R.C., 2008. A reverse transcriptase-polymerase chain reaction survey of infectious bronchitis virus genotypes in Western Europe from 2002 to 2006. *Avian Pathol.* 37 (3), 247–257.
- Xu, Q., Han, Z., Wang, Q., Zhang, T., Gao, M., Zhao, Y., Shao, Y., Li, H., Kong, X., Liu, S., 2016. Emergence of novel nephropathogenic infectious bronchitis viruses currently circulating in Chinese chicken flocks. *Avian Pathol.* 45 (1), 54–65.
- Yang, T., Wang, H.N., Wang, X., Tang, J.N., Lu, D., Zhang, Y.F., Guo, Z.C., Li, Y.L., Gao, R., Kang, R.M., 2009. The protective immune response against infectious bronchitis virus induced by multi-epitope based peptide vaccines. *Biosci. Biotechnol. Biochem.* 73 (7), 1500–1504.
- Zhang, T., Han, Z., Xu, Q., Wang, Q., Gao, M., Wu, W., Shao, Y., Li, H., Kong, X., Liu, S., 2015. Serotype shift of a 793/B genotype infectious bronchitis coronavirus by natural recombination. *Infect. Genet. Evol.* 32, 377–387.
- Zhao, R., Sun, J., Qi, T., Zhao, W., Han, Z., Yang, X., Liu, S., 2017. Recombinant Newcastle disease virus expressing the infectious bronchitis virus S1 gene protects chickens against Newcastle disease virus and infectious bronchitis virus challenge. *Vaccine* 35 (18), 2435–2442.